

# Stress-Shielding Effect of Nitinol Swan-Like Memory Compressive Connector on Fracture Healing of Upper Limb

Q.G. Fu, X.W. Liu, S.G. Xu, M. Li, and C.C. Zhang

(Submitted September 18, 2008; in revised form March 1, 2009)

In this article, the stress-shielding effect of a Nitinol swan-like memory compressive connector (SMC) is evaluated. Patients with fracture healing of an upper limb after SMC internal fixation or stainless steel plate fixation were randomly selected and observed comparatively. With the informed consent of the SMC group, minimal cortical bone under the swan-body and swan-neck was harvested; and in the steel plate fixation group, minimal cortical bone under the steel plate and opposite side to the steel plate was also harvested for observation. Main outcome measurements were taken such as osteocyte morphology, Harversian canal histological observation under light microscope; radiographic observation of fracture healing, and computed tomography quantitative scanning of cortical bone. As a conclusion, SMC has a lesser stress-shielding effect to fixed bone than steel plate. Finally, the mechanism of the lesser stress-shielding effect of SMC is discussed.

**Keywords** fracture healing, internal fracture fixation, nitinol, shape memory alloy, stress-shielding effect

## 1. Introduction

In 1963, Buehler and Wang (Ref 1) from the American Naval Weapon Research Institute reported on the apparent shape memory effect of Nitinol that aroused widespread interest from relevant scholars. Nitinol, with the effect of shape memory and its superiority in wear and corrosion resistance (Ref 2), has been extensively applied in the medical field (Ref 3) and is considered to be a rare “bio-memory material.” Biocompatibility studies have shown NiTi to be a safe implant material (Ref 4, 5). The Chinese scholar, Zhang, has dedicated himself to the study and application of shape memory alloy in the medical field for many years. After intensive research on the physical, chemical, and mechanical nature of Nitinol, and taking into consideration the anatomical characteristics of the long bone, he broke through the traditional concept of internal fixation on fracture and invented the Nitinol swan-like memory compressive connector (SMC) (Ref 6, see Fig. 1a, b, Chinese Patent No. ZL99113873.2) in 1986. By taking advantage of the “thermo-elastic martensite-type” characteristic of Nitinol, the SMC forms the relatively ideal local mechanical environment

necessary for the bio-reaction of the fracture union at the fracture end of the long bone. In addition, the SMC enables persistent and initial axial pressure to be exerted on the fracture end, thereby maintaining a long-term and appropriate initial memory load at the fracture end and preventing the occurrence of osteoporosis and re-fracture (Ref 7, 8).

After fixation of the long bone fracture of the upper limb by either dynamic compressive plate or interlocking intramedullary nail, complications often occur, such as bone nonunion, delayed bone union, or breakage of internal fixator in different proportions. The plate or interlocking nail is typically made of stainless steel, whose rigidity will hinder the process of bone reconstruction, leading to the loss of bone mass and the disorder of bone architecture in the fixed bone segment. Moreover, after the removal of the internal fixator, re-fracture is very likely to occur (Ref 9–11). Clinical treatment of long bone fracture of the upper limb by application of SMC has indicated that under the fixation of SMC, the fracture segment of the fractured bones is connected directly by the lamellar bone, avoiding local external callus and osteoporosis of the cortical bone (Ref 6). In order to further confirm such a bone-healing phenomenon and to clarify its nature, our experiment applied SMC to fix long bone fractures of the upper limb in adults, and after bone-healing, the internal fixators were removed to facilitate x-ray imaging, quantitative scanning computed tomography (CT) (Ref 12, 13) of the cortical bone, and histological observation. Finally, by comparing a SMC fixation group with a stainless steel plate fixation group, the stress-shielding effect of SMC on the fixed segment of the fractured bone was evaluated and is discussed.

## 2. Subjects and Methods

### 2.1 Design

Controlled observation experiment.

This article is an invited paper selected from presentations at Shape Memory and Superelastic Technologies 2008, held September 21–25, 2008, in Stresa, Italy, and has been expanded from the original presentation.

Q.G. Fu, X.W. Liu, S.G. Xu, M. Li, and C.C. Zhang, Department of Orthopedics, Changhai Hospital of Second Military Medical University, Shanghai 200433, China. Contact e-mail: zhangchuncai@vip.sina.com.

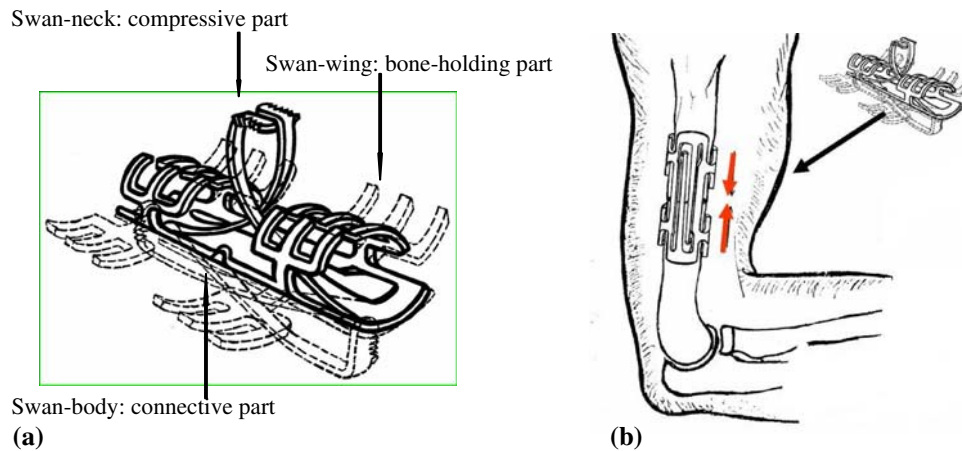


**Fig. 1** (a) Schematic diagram of clinical internal fixation of human long bone fracture by SMC. (b) Schematic diagram of SMC fixating shaft of humerus, the arrow indicate the direction of pressure

## 2.2 Time and Setting

The experiment was performed at the Department of Orthopedics, Changhai Hospital of Second Military Medical University in Shanghai from March 2002 to August 2004.

## 2.3 Participants

Patients with complete healing of bone fracture of the upper limb after SMC internal fixation or stainless steel plate internal fixation were randomly selected. There were 20 cases in the SMC group, including 14 males and 6 females, aged 18-53 years (average = 28.3 years). Their distribution of fracture sites were: eight cases of humerus fracture, one case of ulna fracture, two cases of radius fracture, and nine cases of both ulna and radius fracture. Their time duration from the fracture to the treatment of internal fixation was  $3.92 \pm 1.47$  days. Their time duration from surgery to internal fixator removal was  $11.2 \pm 3.68$  months. There were 20 cases in the stainless steel plate group, including 16 males and 4 females, aged 19-46 years (average = 27.5 years). Their distribution of fracture sites was: 7 cases of humerus fracture, 2 cases of ulna fracture, 1 case of radius fracture, and 10 cases of both ulna and radius fracture. Their time duration from the fracture to the treatment of internal fixation was  $4.16 \pm 1.52$  days. Their time duration from surgery to internal fixator removal was  $12.6 \pm 4.10$  months. All of above fractures were fresh in the upper limbs, received the first internal fixation and achieved complete healing. Both the SMC and the stainless steel plate placed within the body conformed to national standards. According to statistical analysis, there were no significant differences in ages, time duration from the fracture to the treatment of internal fixation, and time duration from surgery to removal of internal fixator between the two groups.

## 2.4 Internal Fixation Device

**2.4.1 The Structure and Functional Mechanism of SMC.** The SMC was invented by Zhang et al. (Ref 6) from the Department of Orthopedics, Changhai Hospital of Second Military Medical University in Shanghai, and produced by Ximai Biological Medical Equipment Corporation (Chinese registration number of the medical equipment: 2002, No. 3040024), complying with the national standards. According to

the anatomical and biomechanical characteristics of the bone shaft of the upper limb, a plate with the width of 1.5-2.5 mm, containing 50-53% of nickel (the other component being titanium) is made with three parts: connective part (a swan-body), compressive part (two swan-necks), and bone-holding part (four swan-wings). The inner diameter of the SMC is 6-23 mm, and the diameter-length ratio is 1:6. It has a one-way orientation and the shape recovery temperature is  $(33 \pm 2) ^\circ\text{C}$ .

Before implantation, the SMC was placed in the 0-4  $^\circ\text{C}$  ice water for cooling, because the Nitinol is formable at lower temperatures (martensitic). The four swan-wings were opened with a needle forceps, so the spreading distance could be larger than the diameter of the fixed bone. The two swan-necks were pulled straight toward the dorsal side of the swan-body. The midpoint of the swan-body was aimed at the fracture site, and two holes were drilled on the fractured bone at the same surface with that of tail of the spread swan-neck—both proximal and distal to the fracture site. After reduction of the fracture, the SMC was inserted, and the tail of the spread swan-neck was then inserted into the holes. Afterward, water at 40-50  $^\circ\text{C}$  was used to warm the SMC in order to exert its mechanical functions. The effect of shape memory of the swan-wings was produced by the patient's body temperature ( $\sim 37 ^\circ\text{C}$ ), and the swan-wings embraced the bone shaft as a ring. Meanwhile, influenced by the tail of swan-neck, the two swan-necks exerted persistent axial pressure on the fracture segment—thus coordinating three-dimensionally to fix the bone shaft (Ref 6).

**2.4.2 The Stainless Steel Plate.** These were imported from other countries but all conformed to national standards.

## 3. Methods

### 3.1 Collection of Samples

Patients with long bone fracture after SMC internal fixation or stainless steel plate internal fixation were selected, and a follow-up showed that the patients had achieved bone-healing. With the patient's permission, a very small quantity of the cortical bone and a small quantity of the normal bone, used as a comparison, were removed when extracting the internal fixation. The positions where the cortical bones were removed

were: under the swan-body and swan-neck of the SMC (Ref 1) and under the steel plate and opposite side to the steel plate (Ref 2).

### 3.2 The Making and Observation of the Light Microscopic Slices

The abovementioned cortical bones were made into light microscopic slices and observed with an Olympus PM-CBK-G biological microscope and photographed.

### 3.3 X-Ray Imaging

Images of bilateral bone shaft were taken 1 week after the removal of the internal fixation, and the conditions of the cortical bone at the broken and the normal parts were compared. Exposure factors were: voltage 50 kV, time 0.1 s, electric current 125 mA, and tube distance 100 cm.

### 3.4 The Quantitative Scanning Computed Tomography of the Cortical Bone

One week after removal of the internal fixation, cross-section scanning with a scanning thickness of 2 mm was carried out by a Somatom CT machine (Siemens Corp., Germany) on the cortical area of 1 cm distance to the center of the broken end. Four small cortical areas were selected randomly at the region of the cortical bone under the plate (the SMC group: cortex under swan-body and under swan-neck of SMC; the stainless steel plate group: cortex under plate and opposite side to plate) after scanning and imaging, and the average CT value of the cortical bone in each small area was automatically calculated by a computer. The average CT value and standard deviation of the cortical bone under the plate were calculated. Meanwhile, the CT value of the corresponding normal bone opposite to the fracture part at the same level was measured as a normal control. To reduce individual variation, the CT value in each group was converted to the percentage form of the normal value.

### 3.5 Main Observatory Indexes

- (1) Histological observations on the osteocyte morphous and Haversian canal were carried out under the light microscope.
- (2) The healing condition of the fractures and state of stress-

shielding were observed from the x-ray images. (3) The CT values of the cortical bones were measured by CT machine.

### 3.6 The Designer, Performer, and Evaluator

All three roles were performed by the author of this article, and nonblind evaluation was used.

### 3.7 Statistical Analysis

Under the direction of faculty in the teaching and research office of statistics at the Second Military Medical University, the author conducted statistical analyses with the aid of SPSS 12.0 software. A difference of  $P < 0.05$  was considered as statistically significant.

## 4. Results

### 4.1 Histological Observation

The histological slices from all cases observed under the light microscope were of lamellar bone structure. Compared with the normal substantia ossea, the manifestations under the connective part and the compressive part of SMC group were not significantly different (see Fig. 2a, b); the lamellar bone had regular architecture, the bone cells in the bone matrix were in good shape, and there was no apparent osteoporosis or bone absorption. In the stainless steel plate group, under the steel plate there was obvious osteoporosis and bone absorption was observed. There were also large or small absorption cavities, expanded Haversian canals, shrinking osteocytes, and enlarged bone lacuna in the lamellar bone (see Fig. 3a). However, the lamellar bone opposite to the steel plate had less severe osteoporosis, less absorption cavities, and less shrinking osteocytes in both percentage and number compared to the substantia ossea under the plate (see Fig. 3b).

### 4.2 X-Ray Imaging Observation

The fracture in all the cases had achieved healing, and the fracture line disappeared. In the SMC group, there was no external callus under the connective part or the compressive part, and the thickness and density of the cortical bone were

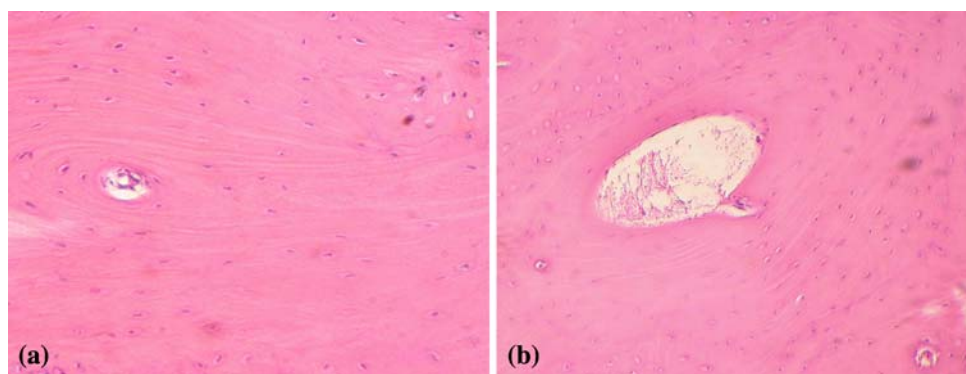


**Fig. 2** (a) Under the body part of SMC, the lamellar bone architecture of the cortical bone was regular, the bone cells in the bone matrix were in good shape, and there was no bone absorption cavity. HE  $\times$  200. (b) Under the compressive part of SMC, the bone substance was similar to that of the normal cortical bone in shape, the lamellar bone architecture was regular, and the bone cells in the bone matrix were in good shape. HE  $\times$  200

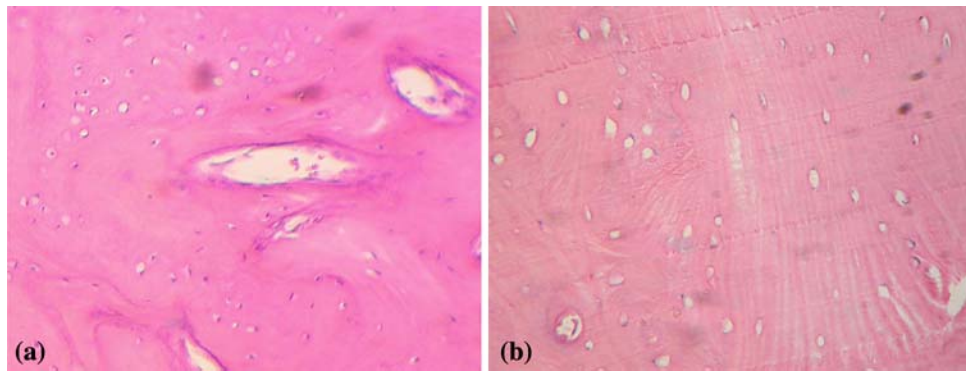


**Fig. 3** (a) Under the steel plate, obvious osteoporosis and absorption were observed, and there were large or small absorption cavities in the architecture of the lamellar bone, expanded Haversian canals, atrophied bone cells and enlarged bone lacunas. HE  $\times 200$ . (b) In the cortical bone opposite to the steel plate, the osteoporosis of the lamellar bone was apparently less severe than that of the bone segment under the plate, and the percentage and the number of the absorption cavities and atrophied bone cells were also less than those of the bone segment under the plate. HE  $\times 200$

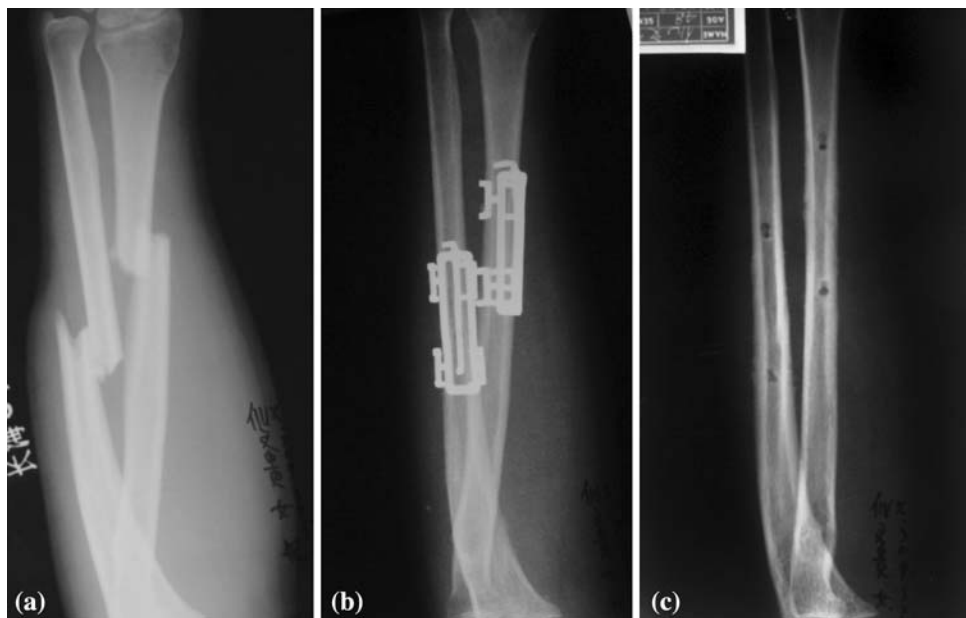


**Fig. 4** (a) Fresh fracture of both the ulna and the radius shaft. (b) The healing conditions of the fracture of the ulna and the radius shaft after fixation of SMC, and there was no formation of external callus. (c) 11 months after the operation, the SMC was removed, and the thickness and density of the cortical bone were similar to those of the normal bone substance

similar to those of the normal bone; the cortical bone was in good shape, and its medullary cavity structure and gray scale had no significant differences compared with those of the normal side, indicating good molding of the bone structures (see Fig. 4a-c). In the stainless steel plate group, under the steel plate there was occasionally a small quantity of external callus, the cortical thickness became thinner, and there were pressure marks of deossification in the lateral side of the cortical bone after the removal of the steel plate. The cortical bone opposite to the steel plate had higher thickness and density than those of the cortical bone beneath the steel plate, the bone densities of the two parts were both slightly lower than that of the normal bone, the medullary cavity was recanalized on the whole. In addition, in some cases the density of the medullary cavity was higher than that of the opposite side (see Fig. 5a-c).

#### 4.3 The Measurement of the CT Values of the Cortical Bone

There were no significant differences in the CT values between the connective part and the compressive part of the SMC group ( $92.9 \pm 6.8\%$  vs.  $93.3 \pm 5.6\%$ ,  $P > 0.05$ ; see Fig. 6a). In the stainless steel plate group, the CT value of the cortical bone under the steel plate was lower than that of the bone opposite to the steel plate, indicating there were significant differences ( $85.3 \pm 5.3\%$  vs.  $91.2 \pm 4.9\%$ ,  $P < 0.05$ ; see Fig. 6b). Comparison between groups showed that the CT values of the two parts in the stainless steel plate group were both lower than the CT values of the two parts in the SMC group ( $P < 0.05$  or  $P < 0.01$ ); the CT value of the cortical bone under the plate was the lowest, the CT value opposite to the steel plate was the lower, while those under the connective



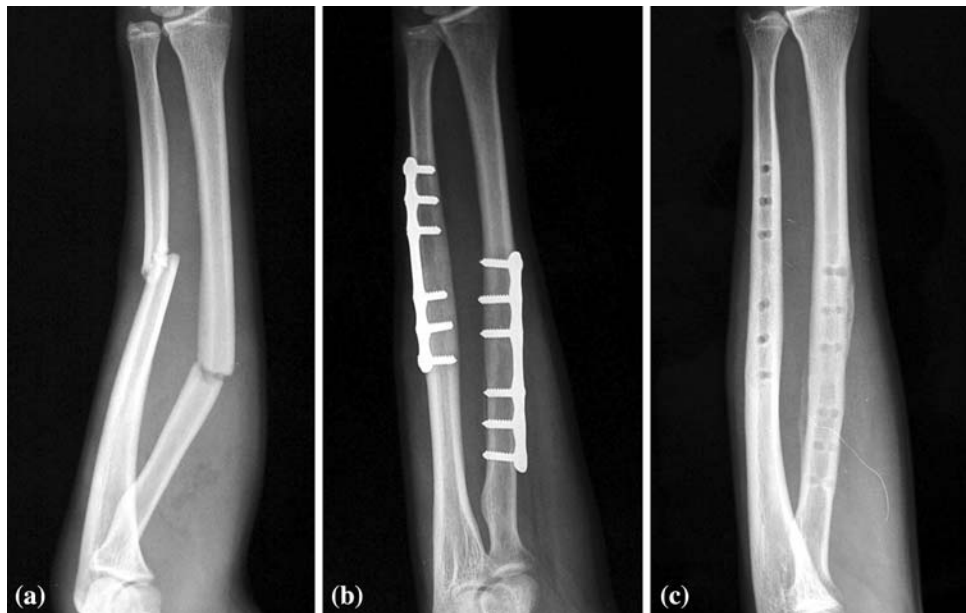


**Fig. 5** (a) Fresh fracture of both the ulna and the radius shaft. (b) The healing conditions of the fracture of the ulna and the radius shaft after fixation of stainless steel plate. There was a small quantity of external callus. (c) 13 months after the operation, the steel plate was removed. The cortical bone absorption under the plate became thinner, and the thickness and density of the cortical bone opposite to the steel plate were higher than those of the cortical bone under the plate

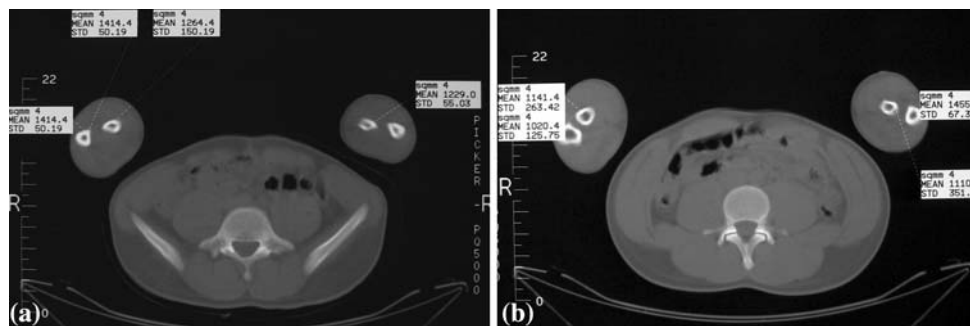


**Fig. 6** (a) After the removal of SMC, CT scan was performed on the area with the original fractured ends of the ulna and the radius shaft as the center, and the average CT value of the specified area was measured and compared with that of the opposite normal bone shaft at the same level. (b) After the removal of the steel plate, CT scan was performed on the area with the original fractured ends of the ulna and the radius shaft as the center

part and the compressive part of SMC were at the same high level.

## 5. Discussion

### 5.1 The Development of Internal Fixation and Stress-Shielding Effect

Bone fracture refers to the consecutive destruction of the bones due to mechanical high force. Its union is a very complicated biological process influenced by many factors, especially a favorable local mechanical environment that is considered as one of the prerequisites to successful union. The importance of the stress environment to the fracture union has been generally recognized (Ref 14). During the treatment of internal fixation for bone fractures, the influence of bone plate on the blood supply of the fractured site should be reduced into

the minimum. In addition, stress stimulation should be exerted on the fracture segment in order to promote bone-healing at the same time as maintaining the stability of the fractured site.

As early as in 1886, Hansmann (Ref 15) from Germany reported the method of treating bone fractures with a plate-screw system. In the past 30 years, the AO School, with Muller et al. (Ref 16) in Switzerland as the leader, established the principle of firm internal fixation that was widely accepted. The firm internal fixation plate can provide stable mechanical environment for the fractured site, ensuring its primary healing. The correct application of firm internal fixation is also conducive to the early exercise of the affected limb, avoiding the occurrence of such complications as myatrophy and ankylosis. However, a large amount of laboratory and clinical experiments have shown that at the advanced period of bone-healing—due to the stress-shielding effect of the bone plate on the fractured part—the local cortical bone lacked physical stimulation and the plate was hence unfavorable for the

reconstruction of the bony callus, leading to local osteoporosis and thinning of the cortical bone. Re-fracture was liable to occur after the removal of the internal fixator.

As is known, when two or more materials with a different moduli of elasticity constitute a mechanical system, a redistribution of force will occur. Consequently, the material with greater modulus of elasticity will support more force, and the material with lesser modulus of elasticity will support less force; the strain will be reduced accordingly. This is called the stress-shielding effect. Due to the comparatively large difference between the modulus of elasticity of the material of the bone plate and the bone tissue, the influence of the firm compressive bone plate on the fixed part of bone is considerable. Cochran et al. (Ref 17) applied an AO compressive steel plate with four holes to fix the femur of dogs and found that after fixation, the average compressive strain of the fixed segment was decreased by 45% (especially that of the cortical bone under the bone plate, which was decreased by 84%). According to our current study and the studies of many other scholars, after firm fixation, the local cortical bone became thinner, some absorption cavities appeared, and the medullary cavity of bones became increasingly larger. In histology, there were large or small absorption cavities, expanded Haversian canals, shrinking osteocytes and enlarged bone lacuna in the bone architecture. The more conspicuous the abovementioned changes, the poorer the mechanical property of the bone will be. Due to the lack of stress stimulation in the fractured site, the cell function (controlled by mechanical environment) will be abnormal, such as a decrease of proliferation of the osteoblast and a delayed appearance of osteoblast, leading to local osteoporosis.

Therefore, the correct application of internal fixation and the reduction of the stress-shielding effect are important factors for improving the quality of bone-healing (Ref 18). At the end of the 1970s, many scholars put forth the concept of nonfirm internal fixation. Animal experiments have confirmed that the low-rigidity bone plate made of compound materials can significantly reduce the osteoporosis caused by the stress-shielding effect. However, this plate was weak in stabilizing the fixed site and had a comparatively high rate of delayed union and nonunion of the fracture. Subsequently, people began to use such absorbable biodegradation materials as polylactic acid and polyglycolic acid to make the bone plate, but the degradation speed was hard to control, and the initial mechanical intensity was also hard to meet the requirements of internal fixation of the long bone fracture.

The ideal bone plate should provide stable mechanical environment at the initial stage of bone-healing, and then decrease gradually, rather than abruptly, its stress-shielding effect, thus ensuring a gradual increase of the stress stimulation to the physiological level at the fracture site, hastening the process of bone-healing and molding and preventing the occurrence of local osteoporosis and re-fracture. To meet these ideal requirements, Zhang et al. invented the Nitinol SMC based on the shape memory effect of Nitinol. It is composed of a connective part (swan-body), two pairs of a horizontal encircling part (swan-wings), and a pair of a longitudinal compressive part (swan-necks). The swan-wings resemble a circle when holding the bone and provide point contact instead of close contact with the uneven bone surface. The swan-necks, driven by the body temperature and assisted by the shape memory effect, exert a persistent and dynamic longitudinal load effect on the fracture segment. The combination of the three

parts of SMC constitutes the 3D fixation of the long bone shaft. The combination of this unique metal material with the geometric structure is, from the angle of biomechanics, conducive to the prevention of osteoporosis and osteanabrosis (Ref 7, 8).

## **5.2 The Relation Between Bone Tissue and Stress**

Some studies (Ref 19) have indicated that changes of the bone structure are closely related to the mechanical properties of the bone. The mechanical environment of the fractured site impacts greatly on the process of bone-healing (Ref 20). Studies on biochemistry and molecular biology have revealed that under proper stress stimulation, the expression level of the related genes will be changed and the cytokine that regulates bone-healing will be produced (Ref 21). The primary callus reaction in the early stage of bone fracture is the basic reaction of bone tissues to injury, and the subsequent bone callus bridging process is closely related to the mechanical factors (Ref 22). In the early stage of bone-healing, the longitudinal compressive stress drives the differentiation of osteoblast and fibroblast into bone tissues, which is beneficial to the bone-healing. The sheering and the torsion of load will produce shear stress force, which drives the fibroblast into fibrous tissues and redistributes the stress within the bone, leading to the over-concentration of layer interface stress of the fractured ends. Thus, it is unfavorable for the healing of fracture (Ref 23) and may directly destruct the newly born capillaries and bone callus. However, in the advanced stage of union, the various stresses are all capable of the reconstruction of bone callus, and the increase of shear stress can promote the differentiation of osteoblast, resulting in more osteoid deposition and the mineralization of bones (Ref 24). If the stress is too small, the mechanical induction of tissue differentiation will be decreased, often resulting in delayed union and nonunion of the bone. If the stress is too large, the reactive surface absorption will take place in the bone-bone interface and the bone-internal fixation interface of the intravital bone, leading to osteanabrosis. When the stress surpasses a specific critical point, further differentiation or union may both stop.

Bone tissue may be functionally adaptive to stress, which ensures its growth in certain directions under the influence or direct action of stress. This is because the changes of stress in the bone tissue can induce the corresponding changes of the electric field, while the changes of the electric field will in turn stimulate the production of the bone tissue. The reaction and the functional adaptation of the bone tissue to the applied load are mainly due to reaction of the bone cell, ossein and bone extracellular fluid to stress or strain caused by the load, constituting a complicated auto-feedback regulatory system within the body. The manifestations are that the bone formation increases at the compressed side due to the stress effect, while bone absorption accelerates at the tension side. However, under certain compressive stress, the re-aggregation and re-absorption of bone tissue are mutually balanced. Additionally, if the compressive stress increases, the bone formation strengthens, and if the compressive stress decreases, the bone re-absorption strengthens (Ref 25, 26).

## **5.3 The Mechanism of Low Stress-Shielding Effect of SMC**

This study has confirmed that the SMC has low or almost no stress-shielding effect on the fixed segment of bone. By comparison of the x-ray images, CT values, and histological

observation results between the SMC group and the steel plate group, it was found that there was osteoporosis of the cortical bone under the plate in the steel plate group, while there was hardly any bone absorption and osteoporosis in the SMC group's cortical bone, suggesting the low stress-shielding effect of SMC on the fractured ends.

The SMC's effective mechanism may lie in the unique property of the nickel-titanium memory alloy and special structure of SMC. The elasticity modulus of the human bone is 7-30 GPa. Compared with stainless steel (183.6 GPa), the elasticity modulus of the nickel-titanium memory alloy (61.7 GPa) is similar to that of the human bone (Ref 27). Hence, the stress-shielding effect that existed in the utilization of medical metal materials is greatly reduced by the utilization of nickel-titanium memory alloy, and the weakening and absorption of bones close to the inserted materials are avoided.

The special structure of SMC forms a unique biomechanical environment at the local fracture site, which is very important for the speed and quality of the bone-healing. (1) The 3D multipoint fixation between the SMC and the fracture segment. The interaction between the standard inner diameter of SMC and the nonstandard outer diameter of the bone shaft forms the 3D multipoint fixation that spreads the pressure produced by the shape memory (Ref 28) and thus avoids the compression of local cortical bone due to the over-concentration of stress. Therefore, there is almost no absorption and atrophy of the bone substance. (2) The persistent longitudinal compressive stress effect on the fracture segment. The longitudinal compressive parts (swan-necks) continuously exert their force value on the anatomical fracture segment. Some studies (Ref 29) found that in the early stage of bone-healing, the compressive stress produced by the longitudinal load can drive the differentiation of osteoblasts and fibroblasts into bones, while in the middle and advanced stages, compressive stress is important to the molding of the fracture. The holistic 3D memory fixation of SMC on the fracture site and the dynamic memory compressive stress are more stable than the screw system and more customized to the bone mechanical behavior. This fixation mode may have the physiological guidance force value which stimulates the bone formation, and is thus bound to influence the process of bone-healing and the molding of bone tissues. (3) The integrative design of SMC forms the holistic effect of the fracture fixation. The device is capable of molding, and the original shape can be resumed, driven by the body temperature after placing into the body. It holds the bone in axial direction and exerts pressure on the fracture segment. These features combine into one and are mutually restricted, forming holistic 3D fixation and dynamic compressive effect that are conducive to the bone-healing and the reconstruction of the bone substance, and can alleviate or avoid the loss of bone substance and osteoporosis due to the stress-shielding effect (Ref 7, 8).

Although the stainless plate has a sliding compressive design, the screw can also provide compressive force for the fracture segment when sliding at the compressive hole. However, this compressive force can only be exerted passively and statically once and is bound to be weakened or disappear following the absorption of the fracture segment. More importantly, due to the apparent difference of the stress environment of the stainless steel plate and the SMC fixation approaches, there are obvious differences in the reconstruction activities of the bone tissue and the degree of the

osteoporosis between these two approaches. Wu et al. (Ref 30) reported the influence of a Nitinol encircling connector and bone plate on the reconstruction of bones, which showed that at the advanced stage of the internal fixation of Nitinol encircling connector, there was less bone absorption, the degree of osteoporosis is less severe, and the speed of its formation is slower. The current experiment confirmed this conclusion.

## 6. Summary

In summary, after fixation of the long bone fracture of adult upper limb by SMC and achieving bone-healing, the internal fixator was removed and x-ray imaging observation, CT scanning of the cortical bone and histological observation were conducted. The results confirmed that the SMC has lesser stress-shielding effect than that of the stainless steel plate, is superior in the period of bone molding, and is helpful for the bone-healing. It is believed that the lesser stress-shielding effect of SMC is related to the special property of Nitinol and the unique geometric structure of SMC, suggesting that new modes of treatment for bone fracture may appear with the improvement of material property and architectonic development of internal fixator.

## References

1. W.J. Buehler and F.E. Wang, A Summary of Recent Research on Nitinol Alloys and Their Potential Application in Ocean Engineering, *Ocean Eng.*, 1968, **1**, p 105-120
2. Y. Oshida and S. Miyazaki, Corrosion and Biocompatibility of Shape Memory Alloys, *Corrosion Eng.*, 1991, **40**, p 1009-1025
3. J.O. Sanders, A.E. Sanders, R. More, and R.B. Ashman, A Preliminary Investigation of Shape Memory Alloys in the Surgical Correction of Scoliosis, *Spine*, 1993, **18**, p 1640-1646
4. A. Kapanen, J. Ryhanen, A. Danilov, and J. Tuukkanen, Effect of Nickel-Titanium Shape Memory Alloys on Bone Formation, *Biomaterials*, 2001, **22**, p 2475-2480
5. M. Assad, N. Lemieux, and C.H. Rivard, Comparative In Vitro Biocompatibility of Nickel-Titanium, Pure Nickel, Pure Titanium, and Stainless Steel: Genotoxicity and Atomic Absorption Evaluation, *Biomed. Mater. Eng.*, 1999, **9**, p 1-12
6. C.C. Zhang, S.G. Xu, J.L. Wang, B.Q. Yu, Q.G. Wang, Q.L. Zhang, Y.T. Liang, and R. Wang, Design and Clinical Application of Swan-like Memory Compressive Connector for Upper Limb Diaphysis, *Acad. J. Sec. Mil. Med. Univ.*, 2001, **22**, p 939-942 (in Chinese)
7. S.G. Xu, C.C. Zhang, J.C. Su, X.H. Liu, Y.N. Wu, J.G. Wu, Z.J. Xue, and Z.Q. Ding, Three-Dimensional Element Analysis of Swan-like Memory Compressive Connector for Treating Fractures and Nonunion of Humerus, *Acad. J. Sec. Mil. Med. Univ.*, 2001, **22**, p 943-945 (in Chinese)
8. S.G. Xu, C.C. Zhang, J.C. Su, W.M. Zeng, S.D. Gu, R.H. Fang, and L.C. Zhang, Biomechanical Study of Swan-Like Memory Compressive Connector for Treating Fractures and Nonunions of Humerus, *Acad. J. Sec. Mil. Med. Univ.*, 2001, **22**, p 946-948 (in Chinese)
9. J.G. Hazenberg, D. Taylor, and T. Clive Lee, Mechanisms of Short Crack Growth at Constant Stress in Bone, *Biomaterials*, 2006, **27**, p 2114-2122
10. S. Tadano and T. Okoshi, Residual Stress in Bone Structure and Tissue of Rabbit's Tibiofibula, *Biomed. Mater. Eng.*, 2006, **16**, p 11-21
11. J. Lin, P.W. Shen, and S.M. Hou, Complications of Locked Nailing in Humeral Shaft Fractures, *J. Trauma*, 2003, **54**, p 943-949
12. C. Bergot, A.M. Laval Jeantet, and K. Hutchinson, A Comparison of Spinal Quantitative Computed Tomography with Dual Energy X-ray Absorptiometry in European Women with Vertebral and Nonvertebral Fractures, *Calcif. Tissue. Int.*, 2001, **68**, p 74-82

13. J.A. MacNeil and S.K. Boyd, Accuracy of High-Resolution Peripheral Quantitative Computed Tomography for Measurement of Bone Quality, *Med. Eng. Phys.*, 2007, **29**, p 1096–1105
14. A.D. Bakker, J. Klein-Nulend, E. Tanck, I.C. Heyligers, G.H. Albers, P. Lips, and E.H. Burger, Different Responsiveness to Mechanical Stress of Bone Cells from Osteoporotic Versus Osteoarthritic Donors, *Osteoporos. Int.*, 2006, **17**, p 827–833
15. C. Hansmann, Eine neue Methode der Fixierung der Fragmente bei omplicierten Frakturen, *Verh. Dtsch. Ges. Chir.*, 1886, **15**, p 134–136
16. M.E. Muller, M. Allgöwer, and H. Willenegger, *Manual der Osteosynthese: AO-Technik*, Springer, Berlin, Heidelberg, 1969
17. G.V.B. Cochran, V.R. Palmieri, and R.E. Zickel, Aramid-Epoxy Composite Internal Fixation Plates: A Pilot Study, *Clin. Biomech.*, 1994, **9**, p 315–322
18. A.P. Datir, Stress-Related Bone Injuries with Emphasis on MRI, *Clin. Radiol.*, 2007, **62**, p 828–836
19. D. Taylor and T.C. Lee, Microdamage and Mechanical Behavior: Predicting Failure and Remodeling in Compact Bone, *J. Anat.*, 2003, **203**, p 203–211
20. O. Akkus and C.M. Rimnac, Cortical Bone Tissue Resists Fatigue Fracture by Deceleration and Arrest of Microcrack Growth, *J. Biomech.*, 2001, **34**, p 757–764
21. D.R. Epari, F. Kandziora, and G.N. Duda, Stress Shielding in Box and Cylinder Cervical Interbody Fusion Cage Designs, *Spine*, 2005, **30**, p 908–914
22. S. Nomura and T. Takano-Yamamoto, Molecular Events Caused by Mechanical Stress in Bone, *Matrix Biol.*, 2000, **19**, p 91–96
23. T.A. Einhorn and J.M. Lane, Significant Advances Have Been Made in the Way Surgeons Treat Fractures, *Clin. Orthop. Relat. Res.*, 1998, **355**(Suppl), p S2–S3
24. K.J. Jepsen, D.T. Davy, and D.J. Krzypow, The Role of the Lamellar Interface During Torsional Yielding of Human Cortical Bone, *J. Biomech.*, 1999, **32**, p 303–310
25. J.P. Lai, G. Wei, X.B. Li, and M. Xie, Research and Design of Bone Plate with Low Stress-shielding Effect, *Orthop. Biomech. Mater. Clin. Study*, 2007, **4**, p 51–52 (in Chinese)
26. W.Z. Xu, Y.J. Wang, X.Z. Xu, L.M. Wang, and Y.J. Wang, Treatment of Femoral Fractures with Stress-Controlled Auto-Compression Locking Nails, *Chin. J. Orthop. Trauma*, 2007, **9**, p 670–674 (in Chinese)
27. J. Rubin, X. Fan, D.M. Biskobing, W.R. Taylor, and C.T. Rubin, Osteoclastogenesis is Repressed by Mechanical Strain in an in Vitro Model, *J. Orthop. Res.*, 1999, **17**, p 639–645
28. Y. Wang, J. Tang, Z.D. Cui, S.L. Zhu, and X.J. Yang, Properties and Bioactive Surface Engineering on Nickel-Titanium Shape Memory Alloy, *Heat. Treat. Metals*, 2004, **29**, p 40–45 (in Chinese)
29. Y.Z. Zhang, Q.X. Wang, J.S. Pan, C.P. Zhang, L.L. Zhao, and Z.H. Song, The Design and Biomechanical Stability of the Automatic Physiological Compression Plate, *Chin. J. Orthop. Trauma*, 2005, **7**, p 66–68 (in Chinese)
30. X.T. Wu, K.R. Dai, and X.S. Zu, et al., The Effect of Internal Fixation of Nitinol Encircling Fixator and Steel Plate on the Healing and Reconstruction of Fracture, *Chin. J. Surg.*, 1998, **33**, p 481–484 (in Chinese)